The Henryville Bed of the New Albany shale—II.
Comparison of the nickel and vanadyl porphyrins in the bitumen with those generated from the kerogen during simulated catagenesis

GARY J. VAN BERKEL[1]*, J. MARTIN E. QUIRKE[2] and ROYSTON H. FILBY[1]

[1]Nuclear Radiation Center and Department of Chemistry, Washington State University, Pullman, WA 99164-1300, U.S.A.
[2]Department of Chemistry, Florida International University, Tamiami Trail, Miami, FL 33199, U.S.A.

Abstract—The Ni(II) and VO(II) porphyrin distributions in the bitumen from the Henryville Bed of New Albany shale (Clark County, Indiana) are compared with those of porphyrins isolated from a single New Albany shale kerogen aliquot by five sequential pyrolyses (110–450°C). Both the bitumen and the pyrolysates contained Ni(II) and VO(II) complexes of at least three skeletal types: deoxophylloerythro-etioporphyrin (DPEP), etioporphyrin (etio), and tetrahydrobenzo-DPEP (THBD). Ni(II) Benzo-DPEP and VO(II) benzo-DPEP and VO(II) benzo type porphyrins were detected in the pyrolysates but not in the bitumen. It was concluded from a comparison of porphyrin distributions in the pyrolysates that porphyrins were liberated from the kerogen by enhanced solubilization and/or desorption into the solvent rather than by kerogen–porphyrin carbon–carbon bond cleavages. Substantial amounts of organically combined nickel and vanadium remain in the kerogen after pyrolysis and may comprise porphyrin and non-porphyrin complexes. The similarity of the porphyrins in the bitumen and the pyrolysates indicates that porphyrins in the bitumen were released as a result of kerogen maturation. The similarity of the Ni(II) etio and DPEP species to the corresponding VO(II) porphyrins indicates that both metal complexes had a common premetallation tetrapyrrole precursor and that this precursor may have been associated with the evolving kerogen.

Key words—nickel, vanadyl porphyrins, oil shale, kerogen, pyrolysis, EI–MS

INTRODUCTION

The geoporphyrins are found in a wide variety of geological environments as mixtures of two major types, etioporphyrins (etio, 1) and deoxophylloerythroetioporphyrins (DPEP, 2), and in smaller amounts, as a variety of other skeletal types (e.g. 3–9). In this paper, the term DPEP will be used to include all porphyrins bearing one isocyclic ring (i.e. cycloalkanoporphyrins, CAP, 2–6) which are indistinguishable by electron ionization mass spectrometry (EI-MS). In sediments, shales, petroleum, and associated source rocks, the porphyrins occur mainly as Ni(II) and VO(II) complexes Treibs, 1936; (Baker and Louda, 1983, 1986a; Filby and Van Berkel, 1987); however, Cu(II) porphyrins and free-base species have been detected in immature sediments (Palmer and Baker, 1973; Baker et al., 1978; Baker and Louda, 1986a). Recent improvements in porphyrin isolation techniques (e.g. Sundararaman, 1985; Barwise et al., 1986; Quirke, 1987) and the determination of the structures of

over 35 geoporphyrins (e.g. Chicarelli et al., 1987; Ocampo et al., 1987) have contributed greatly to the understanding of porphyrin geochemistry, yet many aspects of the origin and evolution of the geoporphyrins remain unresolved. In particular, there has been much speculation as to the role of kerogen in the geochemistry of the porphyrins (Mackenzie et al., 1980; Barwise and Roberts, 1984; Barwise, 1987; Van Berkel and Filby, 1987; Filby and Van Berkel, 1987; Van Berkel, 1987).

Baker and Louda (1983, 1986a) have proposed that, in sediments, Ni(II) porphyrins form from cyclic tetrapyrroles with a limited range of β-substituents as "free" or solvent extractable species. Conversely, they considered the VO(II) porphyrins to form in association with kerogens and to be released to the evolving bitumen only by thermal cracking of kerogen during catagenesis. The geochemical evidence in support of this concept can be summarized as follows:

(i) In general, VO(II) porphyrins are found in sediments which have undergone a moderate degree of thermal stress, whereas Ni(II) porphyrins are common in all but the most recent sediments.

(ii) In sedimentary sequences, high carbon-number porphyrins (etio > C_{33}; DPEP > C_{35}) are predom-

*Present address: Analytical Chemistry Division, Oak Ridge National Laboratory, Oak Ridge, TN 37831, U.S.A.
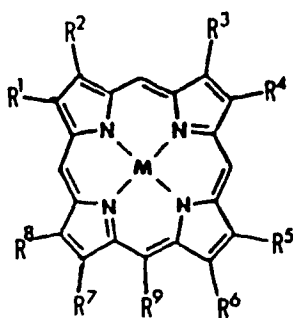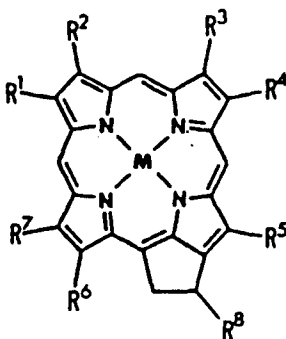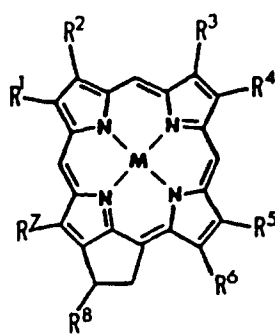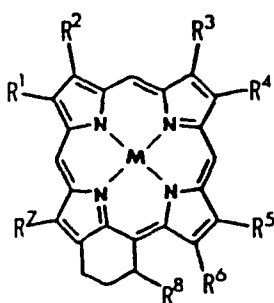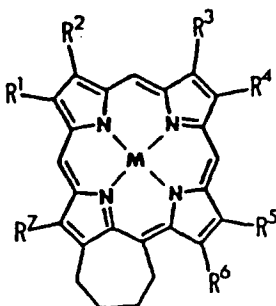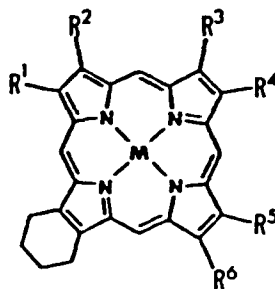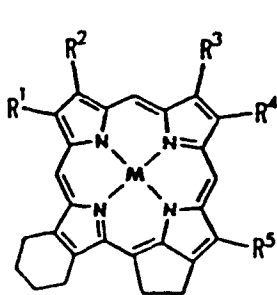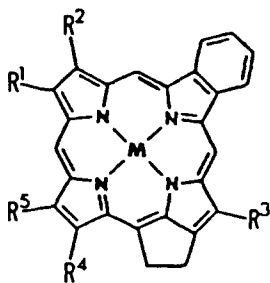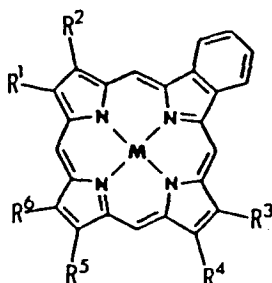
inantly VO(II) porphyrins. There are few reports of Ni(II) porphyrins with carbon numbers greater than C_{33} in sediments (Baker and Louda, 1983, 1986a).

(iii) In the Paris Basin sediments, Mackenzie et al. (1980) showed that there was a marked discontinuity in the variation of porphyrin indices with depth at the zone of oil generation (2100–2450 m). At this point, the total porphyrin concentration, average carbon number, and DPEP/etio ratio all increased. Mackenzie et al. (1980) proposed the generation from kerogen of VO(II) porphyrins with an increased DPEP/etio ratio and with extended alkyl substituents to account for these observations.

(iv) Barwise and Roberts (1984) investigated the effect of catagenesis on porphyrin distributions in the El Lajjun shale (Upper Cretaceous, Jordan) by monitoring samples of increasing thermal maturity across the basin (i.e. samples at increasing depths). They found that the total VO(II) porphyrin content of the bitumen increased in the oil generation window (i.e. during catagenesis) and the concentration of etio porphyrins reached a higher level than the initial porphyrin (mostly DPEP) concentration. Barwise (1987) made a similar observation for a suite of shale samples from the Gulf of Suez. Barwise (1987) concluded from these observations that substantial quan-

tities of etio porphyrins were generated from the kerogen during catagenesis.

(v) Studies on the Cape Verde Rise sediments (Baker *et al.*, 1977; Quirke *et al.*, 1982) revealed that a core section, close to a volcanic intrusion, contained Ni(II) porphyrins (14 ppm) and VO(II) porphyrins (27 ppm). The porphyrin distributions determined by high performance liquid chromatogram (HPLC) resembled those of crude oils (Quirke *et al.*, 1982). In contrast, a deeper core, which was much less influenced by the volcanic intrusion, contained only Ni(II) porphyrins (3.5 ppm) which is typical of thermally immature sediments.

In an experimental investigation of the role of kerogen in porphyrin geochemistry, Van Berkel and Filby (1987) showed that both Ni(II) and VO(II) porphyrins could be generated from the kerogen of the New Albany and Woodford oil shales, thereby providing the first direct evidence of an association between kerogen and metalloporphyrins. These results indicated that the concept of selective kerogen association of VO(II) porphyrins needed to be modified. These experimental observations provide support for a growing body of geochemical evidence that Ni(II) porphyrins, as well as VO(II) porphyrins, are associated with kerogens. For example:

(i) Some kerogens contain concentrations of organically-bound nickel and vanadium that exceed the metalloporphyrin concentrations normally found in bitumens (Van Berkel and Filby, 1988; Van Berkel and Filby, 1987; Van Berkel, 1987; Riley and Saxby, 1982; Spiro *et al.*, 1983). Van Berkel and Filby (1987) have shown that at least part of the organically bound nickel and vanadium in the kerogens of the New Albany and Woodford shales is porphyrinic.

(ii) The Ni/V ratio of the kerogens from several Israeli oil shales, and the Ni(II) and VO(II) porphyrin ratios (NiP/VOP) in the associated bitumens are similar (Spiro *et al.*, 1983). This implies a correlation between the porphyrin content of the bitumen and the nickel and vanadium content of the kerogen.

Defining the role of kerogen in the origin and evolution of the geoporphyrins has been hindered by the lack of studies in which the Ni(II) and VO(II) porphyrins in the bitumen and kerogen of specific source rocks have been compared. Van Berkel and Filby (1987) reported the relative abundances, determined by HPLC, of the VO(II) C_{28} and C_{29} etio and VO(II) C_{31} and C_{32} DPEP porphyrins in the New Albany shale bitumen and kerogen pyrolysates. Few conclusions could be reached on the porphyrin-kerogen association mechanism because data on the entire VO(II) porphyrin arrays and the abundances of the Ni(II) porphyrins were not reported. As a first step towards completion of that study, Van Berkel *et al.* (1989) determined the Ni(II) and VO(II) porphyrin distributions in the New Albany shale bitumen by using EI-MS. From these data it was deduced

that the similarity in the carbon number ranges and C_{max} values for the DPEP and the etio species of both metals indicated common tetrapyrrolic precursors and similar geochemical evolution.

In this paper, the original studies of Van Berkel and Filby (1987) are extended further. The distributions of the Ni(II) and VO(II) porphyrins isolated from the New Albany shale bitumen and those of the porphyrins generated from the New Albany shale kerogen during simulated catagenesis are compared. The porphyrin distributions in the New Albany shale bitumen are discussed in Part I of this study (Van Berkel *et al.*, 1989).

EXPERIMENTAL

Sample

A sample from the Henryville Bed of New Albany shale (Mississippian, Clark County, Indiana) was used in this study. The description of this sample is presented elsewhere (Van Berkel *et al.*, 1989).

Sample preparation

The bitumen extraction, kerogen isolation, and kerogen pyrolysis procedures are outlined in Fig. 1 and discussed in detail elsewhere (Van Berkel, 1987; Van Berkel and Filby, 1987; Van Berkel *et al.*, 1989). The bitumen extracted from the shale by toluene-methanol is designated bitumen I and the bitumen II was extracted by toluene-methanol from the HCl-HF demineralized shale (i.e. kerogen).

Determination of nickel and vanadium in kerogens

Nickel and vanadium concentrations were determined using instrumental neutron activation analysis (INAA; Van Berkel, 1987; Van Berkel and Filby, 1987).

UV–visible spectroscopy

UV–visible spectra were obtained on a Perkin-Elmer Model 320 Spectrophotometer. Solutions of the bitumen and pyrolysates in toluene (0.200 mg/mL) were prepared and metalloporphyrin concentrations estimated using the absorbances at 555 nm ($\epsilon = 33.1$ L mmol^{-1} cm^{-1}) and 570 nm ($\epsilon = 31.6$ L mmol^{-1} cm^{-1}) for Ni(II) and VO(II) porphyrin fractions, respectively (Smith 1975).

Porphyrin isolation

The method for isolation of the Ni(II) and VO(II) porphyrins from the bitumen of the New Albany shale is described elsewhere (Van Berkel *et al.*, 1989). The procedure to isolate the Ni(II) and VO(II) porphyrins from the kerogen pyrolysates is summarized in Fig. 2. The Ni(II) and VO(II) porphyrins were separated from the pyrolysates using heptane/dichloromethane (3:2 v/v) and dichloromethane, respectively, on a silica column. Part of the Ni(II) and VO(II) concentrates were dissolved in dichloromethane and washed successively with 2 M
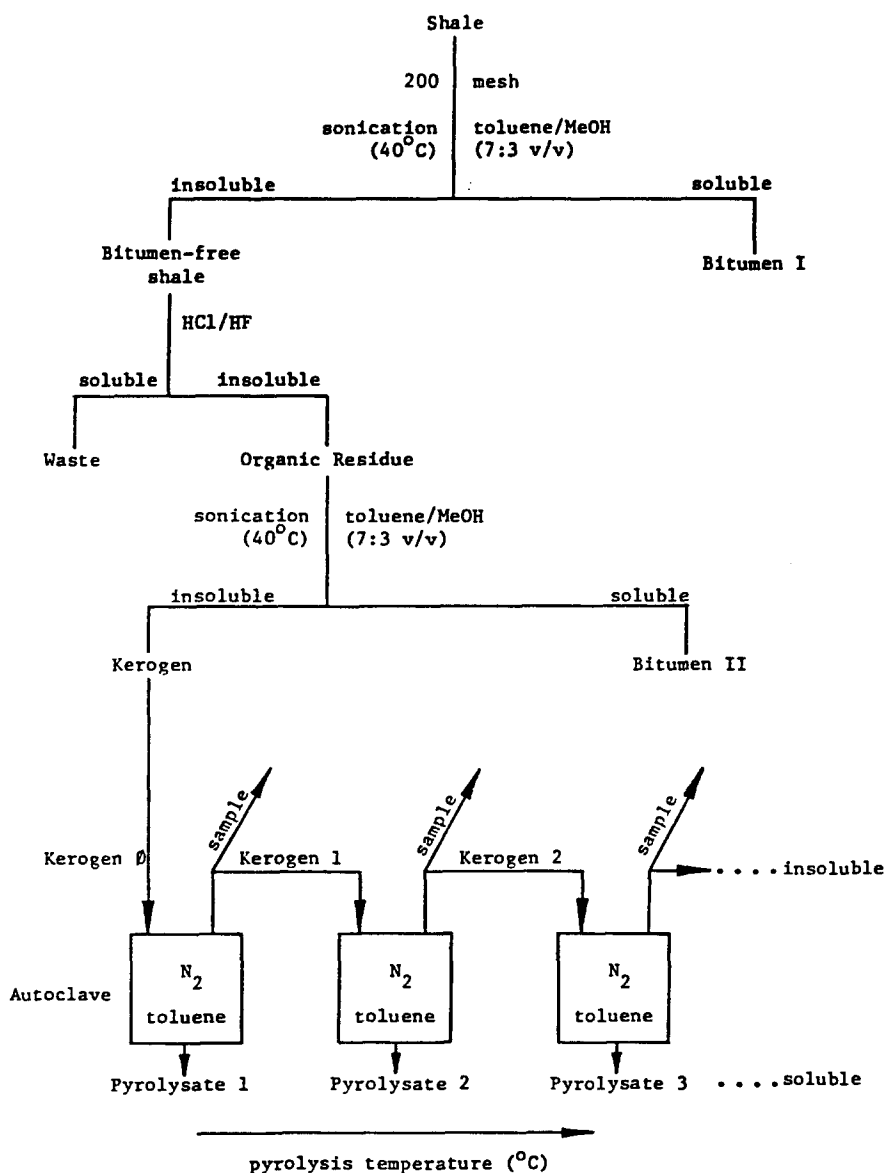
Fig. 1. Sample treatment and sequential pyrolysis of New Albany kerogen.

HCl and 2 M NaOH, and then each was re-chromatographed on silica columns to give purified concentrates for mass spectrometry.

The Ni(II) and VO(II) porphyrin concentrates of pyrolysate 3 were separated into five and six fractions, respectively, by preparative thin layer chromatography (TLC) similar to the method described for the New Albany bitumen (Van Berkel *et al.*, 1989). Although each of the TLC bands was a substantially darker red color than the surrounding area, the fractions were not discrete.

Mass spectrometry

Details of the EI-MS analyses are described elsewhere (Van Berkel *et al.*, 1989). Greater difficulty was encountered in obtaining representative Ni(II) porphyrin mass spectra (particularly for the DPEP

series) for the pyrolysates than for the bitumen. This was due in part to the greater difficulty or purifying the Ni(II) porphyrins because of their lower polarity in chromatographic separations than the corresponding VO(II) species. Thus, strong interactions between the Ni(II) DPEP porphyrins and the remaining impurities (components of the pyrolysates) appeared to modify the volatilization of the porphyrins from the sample crucible.

RESULTS AND DISCUSSION

Pyrolysate and metalloporphyrin yields

The bitumen content of the New Albany shale, pyrolysate yields, nickel and vanadium concentrations of the kerogens, and the yields of nickel and vanadium species from pyrolysis are shown in Table
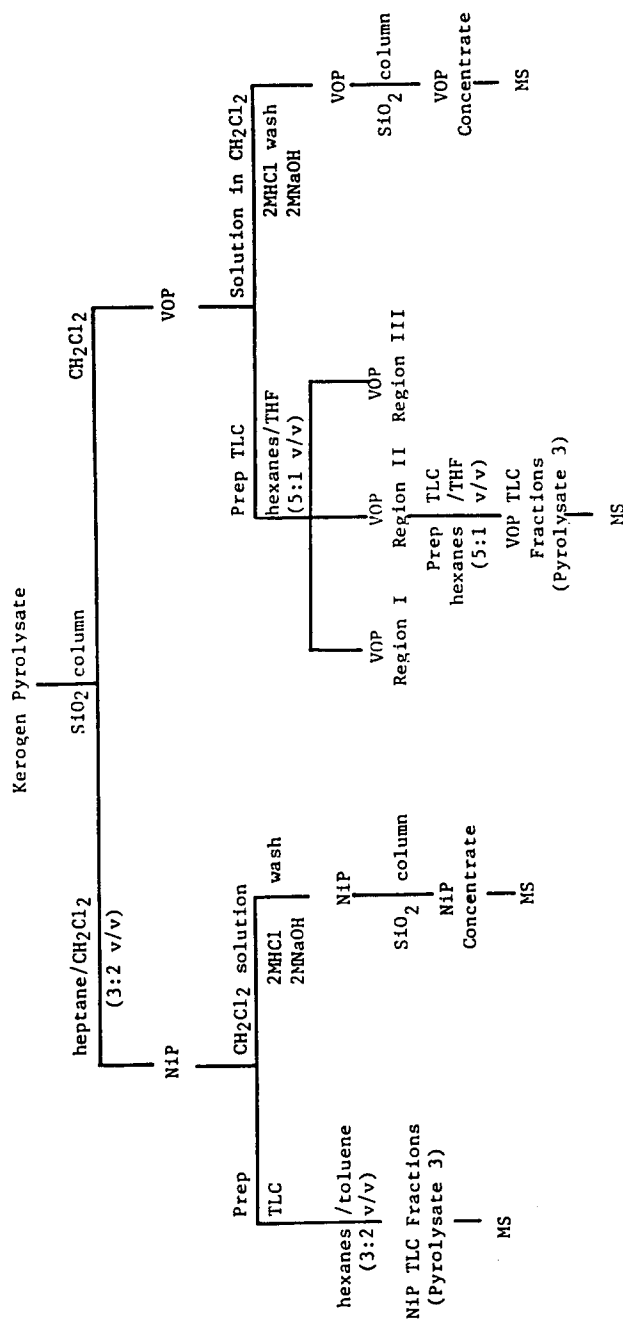
Fig. 2. Scheme for isolation of Ni(II) and VO(II) porphyrins from New Albany pyrolysates.

Table 1. Pyrolysis data and nickel and vanadium concentrations in New Albany kerogen and pyrolysates[a]

Sample	Pyrolysis temperature (°C)	Pyrolysate (bitumen) Yield[b]		Yield of metal Species (μg M_p/μg M_L) 100[b]		Pyrolysate (bitumen) Ni/V (molar)	$[Ni]_{MFK}$ μmol/g[c]	$[V]_{MFK}$ μmol/g	$[Ni/V]_{MFK}$[d]
		(g/g TOC)100	(g/g)100	Ni[c]	V[c]				
Bitumen I	—	(5.44)	(1.2)	—	—	1.00	36.3	13.7	2.65
Bitumen II	—	(1.49)	(0.33)	—	—	1.47	36.3	13.7	2.65
Pyrolysate 1	110	0.24	0.16	0.10	0.18	1.41	37.3	13.1	2.84
Pyrolysate 2	210	1.01	0.70	0.81	0.83	2.78	37.6	13.3	2.84
Pyrolysate 3	300	5.65	3.90	3.7	3.3	3.15	39.0	14.3	2.72
Pyrolysate 5	400	16.6	12.0	5.2	4.7	2.90	46.5	16.3	2.85
Pyrolysate 6	450	26.1	18.9	0.6	0.3	6.21	53.4	16.7	3.19
				(Σ = 10.4)	(Σ = 9.3)				

Σ = 9.3

[a]Conditions: kerogen pyrolyzed for 5 hr at temperature indicated in toluene solvent.
[b]Pyrolysate yields calculated per g TOC in starting kerogen. In the case of the bitumen I and II, yields are per g TOC of shale and of demineralized shale, respectively.
Yields of Ni and V species calculated as [(μg Ni or V in the pyrolysate, M_p)/(μg Ni or V in initial kerogen, M_k)]100.
[c]Ni and V molar concentrations calculated on mineral-free basis (MFK) for starting kerogen (original kerogen in case of bitumens). Relative standard deviations of value are approx. ±4%.
[d]$[Ni/V]_{MFK}$: molar ratio. Relative standard deviation of values approx. ±6%.

1. The bitumen extraction and pyrolysis procedure allowed a distinction to be made among the bitumen extractable from the shale with toluene–methanol (bitumen I), the bitumen strongly associated with the mineral matrix or kerogen which can only be removed after demineralization (bitumen II) and the bitumen generated from the maturing kerogen (i.e. pyrolysates). The bitumens I and II account for approx. 1.2 wt% and 0.33%, respectively, of the New Albany shale (0.054 and 0.015 g/g shale TOC, respectively).

The pyrolysates generated between 100 and 450°C simulate the bitumen which is generated from the kerogen during progression from catagenesis to metagenesis in the geological environment. Although kerogen catagenesis may be considered as maturation of the kerogen involving heteroatom–carbon or carbon–carbon bond cleavage (Tissot and Welte, 1984), much of the material generated by pyrolysis at less than 350°C probably results from increased swelling and solubilization of the kerogen in toluene as has been suggested by McKay (1984) for pyrolysis of the Green River shale. The low temperature (110 and 210°C) pyrolyses give very low yields (0.24 and 1.0 g/g kerogen TOC, respectively). These pyrolysates probably comprise soluble or adsorbed organic matter associated with the kerogen, since in the absence of catalytic mineral matter, carbon–carbon bond cleavage is unimportant at these temperatures. The increasing yield of the pyrolysates with increasing temperature (Table 1) is probably due to a combination of increased kerogen solubility and rupture of weaker bonds. At higher temperatures (i.e. 400 and 450°C) the yield of the pyrolysate is increased considerably by thermal degradation of the kerogen and possibly by decomposition products of toluene. At 450°C, the temperature is sufficiently high to cause severe thermal decomposition of kerogen constituents which is evident from the different nature of the products (predominantly light oils, gases) compared to the pyrolysates obtained at lower temperatures.

The nickel and vanadium concentrations (determined by INAA) in the kerogens at each pyrolysis
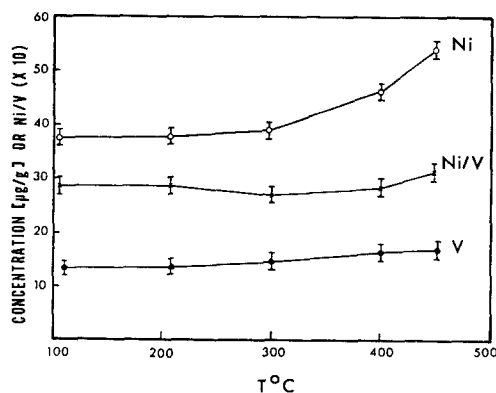

Fig. 3. Variation of Ni and V concentrations (μg/g) and Ni/V ratios in New Albany kerogens.
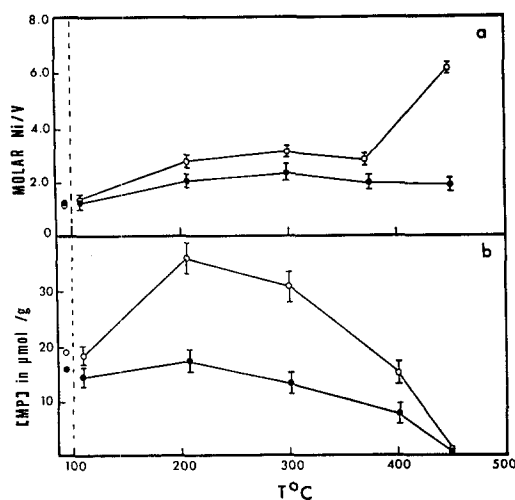
Fig. 4. Variation with pyrolysis temperature of (a) molar ratio of Ni/V (O) and Ni(II) porphyrin/VO(II) prophyrin (●) in pyrolysates, (b) Ni(II) porphyrin (O) and VO(II) porphyrin (●) concentrations (μmol prophyrin/g) in pyrolysates. Points to left of dotted line represent bitumen I values.

Fig. 5. Variation of Ni(II) porphyrin (O), and VO(II) porphyrin (●) yields (μmol porphyrin/g kerogen TOC), and pyrolysate yields (--●--, g pyrolysate/g kerogen TOC) as a function of pyrolysis temperature.

stage were computed as "mineral-free" kerogen (MFK) values (Van Berkel and Filby, 1987) and refer to the concentrations of these elements in organic combination. It is not possible, however, to determine the fraction of the organically bound metals present as porphyrin species from these data. The variation in nickel and vanadium contents of the kerogens with temperature are shown in Fig. 3. As pyrolysis progresses, the nickel concentrations of the kerogen increase, but the vanadium contents and the Ni/V ratios remain constant within experimental error. The small variations in nickel and vanadium concentrations in the kerogen with increasing pyrolysis temperature result from the fact that only a small fraction of the organic nickel and vanadium species in the kerogen is converted to soluble form during pyrolysis. Table 1 shows that, cumulatively, 10.4% of the nickel and 9.3% of the vanadium is removed from the kerogen during pyrolysis. It can also be seen in Table 1 that, up to 300°C, the weight percent yields of nickel and vanadium from the kerogen parallel the weight percent pyrolysate yields. This observation is consistent with a pyrolysis model in which
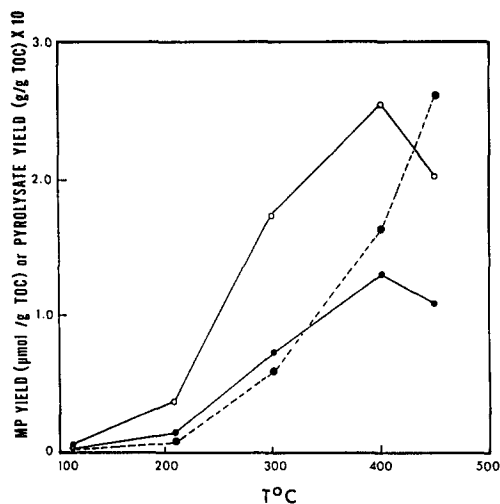
increased solubilization of kerogen, including the metal–organic species, is predominent. Above 300°C, the pyrolysate yield increases relative to the nickel and vanadium yields because kerogen decomposition via carbon–carbon bond rupture becomes significant. At 450°C, metagenetic effects result in a large pyrolysate yield but small nickel and vanadium yields. It is likely that at these high temperatures, the organic nickel and vanadium complexes (including the porphyrins) are thermally degraded, or demetallated, possibly by reaction with H_2S (Rankel, 1987), and the products are retained as insoluble species in the kerogen.

The concentrations of Ni(II) and VO(II) porphyrins in the pyrolysates are shown in Table 2 and Fig. 4b. The concentrations of Ni(II) and VO(II) porphyrins in the pyrolysate 1 are similar to those in the bitumen I. The Ni(II) and VO(II) porphyrin concentrations in the pyrolysate reach maximum values at 210°C and then decrease. With increasing temperature, the yields of Ni(II) and VO(II) porphyrins/g kerogen TOC, shown in Fig. 5, increase up to 400°C and then decrease at 450°C. Thus, as the kerogen is solubilized and/or thermally degraded, metalloporphyrins are released, but above 400°C

Table 2. Metalloporphyrin concentrations in New Albany bitumen and kerogen pyrolysates

Sample	Pyrolysis temperature, °C	Porphyrin concentrations[a]		
		[NiP] μmol/g	[VOP] μmol/g	[NiP]/[VOP] (molar)
Bitumen I	—	19.6	17.4	1.12
Bitumen II	—	7.95	11.1	0.72
Pyrolysate 1	110	18.1	14.2	1.27
Pyrolysate 2	210	36.3	17.4	2.09
Pyrolysate 3	300	31.7	13.4	2.37
Pyrolysate 5	400	15.6	7.91	1.97
Pyrolysate 6	450	1.51	0.79	1.87

[a]Metalloporphyrin concentrations based on absorbances at 550 nm (ϵ = 33.1 L mmol^{-1} cm^{-1}) and 570 nm (ϵ = 36.1 L mmol^{-1} cm^{-1}) for NiP and VOP, respectively, in toluene solvent.

the generation of both bitumen-type material and metalloporphyrins from the kerogen increases with temperature but that the relative release of porphyrins compared to bitumen generation decreases with temperature above 200–300°C. The observation is consistent with a release of porphyrins via increased solubilization or rupturing of relatively weak bonds (e.g. axial ligand–metal ion bonds) together with increased solubilization of the kerogen and increasing thermal degradation of the kerogen with temperature. In the absence of mineral catalysts, carbon–carbon bond scission is probably a minor release mechanism for components of the pyrolysates and for the porphyrins at 300°C or less. At 450°C porphyrin yields decrease because they are being thermally degraded or demetallated.

The Ni/V and NiP/VOP ratios of the pyrolysate generated at 110°C are equal within experimental error to the corresponding values in bitumen I but are significantly less than the Ni/V ratio in the kerogen (Fig. 4a and Table 1). Between 200 and 400°C, the Ni/V ratios of the pyrolysates are similar to the corresponding kerogen values but are higher than the NiP/VOP ratios (Table 2). Thus, a larger fraction of the nickel species in the pyrolysates is non-porphyrinic (or behaves as such) compared to the vanadium species. The much higher value of the Ni/V ratio than the NiP/VOP ratio in pyrolysate 6 (6.21 vs 1.91) indicates that a much larger fraction of non-porphyrin nickel species is generated at 450°C. This does not appear to result from increased degradation of Ni(II) porphyrins relative to vanadium complexes because the NiP/VOP ratio remains constant (within experimental error) between 110 and 450°C (Fig. 4a).

Distribution of nickel and vanadyl porphyrins in the New Albany bitumen and pyrolysates

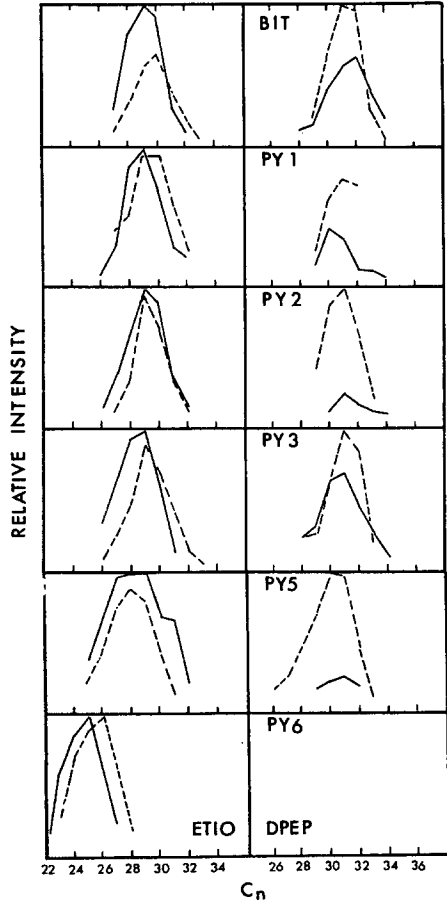The Ni(II) and VO(II) porphyrin distributions in the porphyrin concentrates of the bitumen I and the

Fig. 6. Distribution of Ni(II) etio and Ni(II) DPEP (solids lines) and VO(II) etio and VO(II) DPEP (dashed lines) porphyrins of carbon number, C_n, in New Albany bitumen and pyrolysates. Most abundant pseudo-homolog of each metal series ≡ 100%.

thermal decomposition of the porphyrins is severe and the yield/g TOC decreases (i.e. metagenetic effects). The trends noted in Figs 4 and 5 suggest that

Table 3. Summary of the mass spectral data for the total nickel and vanadyl porphyrin mixtures isolated from New Albany shale bitumen I and New Albany shale kerogen pyrolysates

Sample	Porphyrin	Carbon number range		Major component	DPEP[a] etio	Weighted average mass[b] M	
		etio	DPEP			DPEP	etio
Bitumen I	Ni	C_{27}–C_{32}	C_{28}–C_{34}	C_{29} etio	0.91	522	493
	VO	C_{27}–C_{33}	C_{29}–C_{34}	C_{31} DPEP	1.39	529	510
Pyrolysate 1[c]	Ni	C_{26}–C_{33}	C_{28}–C_{34}	C_{29} etio	0.39	517	494
	VO	C_{27}–C_{32}	C_{29}–C_{32}	C_{29} etio	0.65	525	507
Pyrolysate 2	Ni	C_{25}–C_{31}	C_{30}–C_{34}	C_{29} etio	0.31	529	493
	VO	C_{27}–C_{32}	C_{29}–C_{33}	C_{31} DPEP	1.22	524	508
Pyrolysate 3	Ni	C_{26}–C_{31}	C_{28}–C_{34}	C_{29} etio	0.79	512	481
	VO	C_{26}–C_{33}	C_{28}–C_{33}	C_{31} DPEP	1.11	524	506
Pyrolysate 5	Ni	C_{25}–C_{31}	C_{29}–C_{32}	C_{28-29} etio	0.19	501	482
	VO	C_{25}–C_{31}	C_{26}–C_{33}	C_{30} DPEP	1.10	510	486
Pyrolysate 6	Ni	C_{22}–C_{27}	n.d.[d]	C_{25} etio	0	n.d.	430
	VO	C_{23}–C_{28}	n.d.	C_{26} etio	0	n.d.	451

[a]Obtained by $\Sigma I_{DPEP}/\Sigma I_{etio}$ from background subtracted and isotope (^{13}C, ^{60}Ni) corrected molecular ion intensities, I. DPEP = 2, 3–6 and all other potential cycloalkanoporphyrins.
[b]Obtained by $\Sigma IM/\Sigma I$, where M is porphyrin mass and I is corrected normalized intensity.
[c]Pyrolysate 1 also contained Ni(II) THBD porphyrins of the following carbon numbers (abundances relative to C_{29} etio = 100) C_{31}(6.7); C_{32}(19); C_{33}(19); C_{34}(11). Pyrolysate 1 also contained the VO(II) BD species of carbon numbers (intensities relative to C_{29} etio = 100), C_{38}(31); C_{39}(41); C_{40}(15).
[d]Not detected.

pyrolysates determined by EI-MS are summarized in Table 3. The DPEP and etio distributions are compared in Fig. 6. The Ni(II) and VO(II) porphyrin concentrates of bitumen I and pyrolysate 3 were separated into chromatographic fractions by TLC in order to identify minor components which could not be detected in the mass spectra of the concentrates. Pyrolysate 3 was chosen for further investigation because of the high concentration of porphyrins (31.7 and 13.4 μmol/g for Ni(II) and VO(II) porphyrins, respectively) and because thermal alteration of the porphyrins at 300°C is probably minimal.

(a) Nickel porphyrins. The DPEP and etio species are the major porphyrins detected in the Ni(II) porphyrin concentrate of the bitumen and pyrolysates, except for pyrolysate 6 (450°C) in which only etio species can be detected. The Ni(II) porphyrin concentrate of pyrolysate 1 contained measurable quantities of Ni(II) THBD porphyrins which appear to be much less abundant in the other pyrolysates (Table 3). The higher concentration of THBD porphyrins in pyrolysate 1 relative to the higher temperature pyrolysates suggests that the THBD porphyrins are associated with the mineral matrix of the shales and hence concentrated in bitumen II. The amount of bitumen II recovered, however, was insufficient for analysis of the metalloporphyrins by EI-MS.

Figure 6 shows that the major component in the Ni(II) prophyrin mixtures of each pyrolysate is always etio. The DPEP/etio ratios of the Ni(II) porphyrins in pyrolysates 1 and 2 are similar (0.39 and 0.31, respectively) and the ratio increases to 0.79 at 300°C. At 400 and 450°C the ratio drops to 0.13 and 0, respectively. The increase in the DPEP/etio ratio between 210 and 300°C indicates a preferential release of DPEP porphyrins at 300°C relative to the lower temperature pyrolysates. However, above 300°C the rapid decrease in the relative abundances of DPEP porphyrins may be due to thermal degradation. It should be noted, however, that the DPEP abundances include all CAP porphyrins. It is thus

impossible to determine whether some isomers are preferentially released, or degraded, with increasing temperature.

The observed Ni(II) etio porphyrin distributions of the pyrolysates and the bitumen change very little with increasing temperature up to 400°C. A significant decrease in C_{max}, however, is observed between 400 and 450°C (from C_{28-29} to C_{25}). Although there is little change in the carbon number range between bitumen I and pyrolysates 1 through 3, the etio distribution of pyrolysate 5 (C_{25}–C_{32}) is broader relative to pyrolysate 3 (C_{26}–C_{31}). The broadening appears to be due to the addition of C_{30}–C_{32} etio porphyrins. The anomalously high C_{31} etio abundance and the extended distribution may have resulted from the conversion of the C_{30}–C_{32} DPEP species, which are abundant at 300°C but have virtually disappeared at 400°C, to etio species. These data, although suggestive, cannot be interpreted as unequivocal evidence for a DPEP to etio conversion because a corresponding effect is not seen with the VO(II) porphyrins. The C_{max} of the Ni(II) etio porphyrin distribution is sharply reduced in pyrolysate 6 probably as a result of thermal dealkylation as indicated by the generation of very low carbon number porphyrins (e.g. C_{22}). There is no evidence for the generation of substantial amounts of high carbon number Ni(II) etioporphyrins (viz. $>C_{33}$) from the kerogen.

The carbon number ranges of the DPEP porphyrins in bitumen I are very similar to those of the 110–400°C pyrolysates. There is no systematic shift in the DPEP porphyrin distributions towards lower carbon number DPEP porphyrins with increasing temperature. High carbon number DPEP geoporphyrins (i.e. $>C_{35}$) were not detected in any of the prophyrin concentrates of the pyrolysates.

The carbon number distributions and relative abundances of the Ni(II) porphyrins in the TLC fractions of pyrolysate 3 are summarized in Table 4 and the DPEP and etio distributions are shown in Fig. 7. Fractionation of the Ni(II) porphyrins al-

Table 4. Summary of mass spectral data for TLC fractions of Ni(II) and VO(II) porphyrins isolated from pyrolysate 3 (300°C) of New Albany kerogen

| TLC fraction | Porphyrin type | R_f range | Carbon number range[a] | | | | Major[a] component | DPEP etio |
			etio	DPEP	THBD	BD		
A	Ni	0.48–0.56	C_{24}–C_{29}	C_{28}–C_{30}			C_{26} etio	0.30
	VO	0.38–0.47	C_{26}–C_{30}	C_{28}–C_{32}			C_{27} etio	0.67
B	Ni	0.58–0.63	C_{26}–C_{30}	C_{28}–C_{32}	tr[b]	C_{33}–C_{36}	C_{28} etio	0.90
	VO	0.48–0.52	C_{27}–C_{31}	C_{29}–C_{32}			C_{28} etio	0.69
C	Ni	0.66–0.71	C_{26}–C_{32}	C_{29}–C_{33}	C_{31}–C_{34}	C_{34}–C_{36}	C_{31} DPEP	1.1
	VO	0.53–0.58	C_{28}–C_{32}	C_{30}–C_{33}			C_{29} etio	0.80
D	Ni	0.72–0.75	C_{28}–C_{32}	C_{30}–C_{34}			C_{30} etio	0.30
	VO	0.59–0.62	C_{30}–C_{33}	C_{31}–C_{34}	C_{33}–C_{34}		C_{30} etio	1.01
E	Ni	0.76–0.81	C_{28}–C_{33}	C_{30}–C_{34}			C_{32} DPEP	1.5
	VO	0.63–0.68	C_{31}–C_{34}	C_{32}–C_{35}			C_{32} etio	0.51
F[c]	VO	0.69–0.74	C_{33}–C_{34}	—	—	C_{35}–C_{36}	C_{33} BE[c]	

[a]Intensities are of molecular ions calculated from background subtracted, isotope corrected mass spectra. Major component is 100% intensity in renormalized mass spectrum. DPEP = 2; 3–6; THBD = tetrahydrobenzoDPEP; BD = benzoDPEP; BE = benzoetio.
[b]Traces of C_{31}–C_{32}Ni(II) THBD porphyrins observed in mass spectrum.
[c]Fraction F obtained only for VO(II) porphyrins. Fraction F also contained C_{31}–C_{33}VO(II) BE porphyrins. C_{33}VO(II) BE is major component in this fraction.
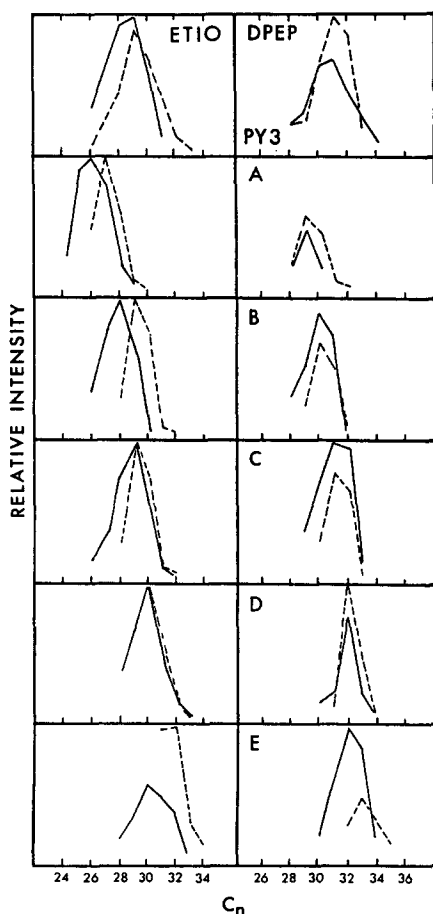
Fig. 7. Distribution of Ni(II) etio and Ni(II) DPEP (solid lines) and VO(II) etio and VO(II) DPEP (dashed lines) porphyrins of carbon number, C_n, in pyrolysate 3 (300°C) and TLC fractions.

lowed the detection of several minor components which were not previously detected. These components were a higher molecular weight DPEP (C_{34}) porphyrin, THBD prophyrins (C_{31}–C_{34}) and benzo-DPEP porphyrins (C_{33}–C_{36}). Benzo-DPEP and THBD porphyrins were detected in fractions B and C. It appears that the primary modes of separation into TLC fractions are based on skeletal type and carbon number. Thus fraction A, the most polar fraction, contained the lowest carbon number etio (C_{24}) and DPEP (C_{28}) components and fraction E, the least polar, contained the highest carbon number etio (C_{33}) and DPEP (C_{34}) species. Nickel porphyrins of several carbon numbers occurred in three or more fractions (e.g. C_{29}–C_{33} DPEP, C_{26}–C_{31} etio). This may be attributed to a combination of factors, including the distribution of a porphyrin component between two or more fractions, and the presence of porphyrin isomers of different polarity. Clearly, the porphyrins of carbon numbers distributed over the greatest number of fractions (C_{28}, C_{29} etio; C_{30} DPEP) are the most likely components to occur in a variety of isomeric forms. The Ni(II) porphyrins of Gilsonite

(an Eocene bitumen) exhibited similar behavior in TLC (Quirke et al., 1979).

(b) Vanadyl porphyrins. The mass spectrometric data for the VO(II) porphyrins in the porphyrin concentrates of the bitumen and pyrolysates are summarized in Table 3 and the etio and DPEP (including all isomeric CAP species) distributions are compared in Fig. 6. Only DPEP and etio porphyrins were detected in the pyrolysates except for pyrolysate 1 which contains significant amounts of benzo-DPEP components. Except for pyrolysate 1 in which the C_{30} etio porphyrin is the major species, and for pyrolysate 6 in which the DPEP porphyrins are absent, VO(II) DPEP porphyrins are the more abundant species in the bitumen I and the pyrolysates. Between 110 and 400°C, the DPEP/etio ratio remains constant, within experimental error, and is not significantly different from the DPEP/etio ratio in bitumen I. Therefore, unlike the Ni(II) porphyrins, the VO(II) porphyrins generated from the kerogen do not show a significant variation in the relative amount of DPEP porphyrin generated as pyrolysis temperature increases. The variation of true DPEP (2), however, cannot be determined because all isomeric CAP porphyrins are included in the DPEP measurement.

The etio porphyrin distributions are very similar for bitumen I and pyrolysates 1–5 and extend to lower carbon number (C_{26}–C_{28}) than the DPEP components of the pyrolysates. Although there is a shift of one carbon number lower in the etio distributions between 100 and 400°C, the only major variation occurs between 400 and 450°C, i.e. pyrolysate 6. The narrower range (C_{23}–C_{28}) and lower C_{max} value (C_{26}) of the distribution at 450°C may be attributed to the effect of metagenesis, i.e. a combination of thermal destruction and dealkylation, as observed for the Ni(II) etio species. High carbon number ($>C_{33}$) etio porphyrins were not generated in significant quantities from the kerogen during pyrolysis.

The carbon number ranges of the DPEP porphyrins in bitumen I and pyrolysates 1–5 are very similar, except in the case of pyrolysate 1 in which no carbon numbers greater than C_{32} are observed. The C_{max} for the DPEP porphyrins decreases from C_{31}–C_{32} for bitumen I to C_{30} for pyrolysate 5. There is no evidence for the generation of substantial amounts of higher carbon number ($>C_{35}$) VO(II) DPEP porphyrins from the kerogen.

The C_{38}–C_{40} VO(II) benzo-DPEP porphyrins, which were detected in pyrolysate 1 only (Table 3), are of considerable interest. The EI-MS fragmentation pattern of these components displayed no $(M-15)^+$ peaks (typical fragments for most geo-porphyrins) which would indicate that they have no ethyl substituents. It is likely that these components are similar to a series of C_{37}–C_{43} "benzo-DPEP" porphyrins detected in Boscan oil (Quirke et al., 1989). The Boscan "benzo-DPEP" porphyrins generated no fragment ions in either conventional EI-MS or in MS/MS spectra, and are clearly very different

from the more typical geoporphyrins. It is unlikely that the VO(II) benzo-DPEP porphyrins in the New Albany sample are generated by carbon–carbon bond rupture from kerogen since they were only detected in pyrolysate 1 which was isolated under mild thermal conditions (110°C). Support for a non-catagenic origin of these porphyrins is provided by the fact that metal-free BD and THBD porphyrins have been detected in immature sediments previously (Baker and Louda, 1986b). Therefore, given that porphyrins are highly surface active molecules (Moore and Dunning, 1955), the presence of a catalytic matrix may have played a significant role in the generation of these unusual geoporphyrins at low temperatures.

The mass spectral data on the TLC fractions of the VO(II) porphryins are summarized in Table 4 and the DPEP and etio distributions are compared in Fig. 7. The VO(II) porphyrins behaved similarly to the Ni(II) porphyrins on the TLC plates. Thus, the most polar fraction (A) had the lowest carbon number DPEP and etio components. In addition, VO(II) porphyrins of several carbon numbers were present in at least three fractions (C_{30}–C_{33}; C_{28}–C_{33} etio). The C_{30} and C_{31} etio porphyrins, which occur in four fractions, are the most widespread etio components, and the C_{32} DPEP, which occurs in all five chromatographed fractions, is the most broadly distributed DPEP component. As is the case for the Ni(II) porphyrins, the distribution of the VO(II) species among several fractions probably results from the chromatographic spreading of the porphyrin component over several fractions and/or the presence of structural isomers of varying polarity. The fractionation of the VO(II) porphyrin mixture allowed several minor components (C_{26} etio; C_{34} THBD; C_{31}–C_{33} benzo-DPEP; C_{36} benzo-etio porphyrins) to be observed which were not detected in the mass spectrum of the mixture. The distributions of DPEP and etio porphyrins in the TLC fractions of pyrolysate 3 are similar to those in the TLC fractions separated from the bitumen I (Van Berkel et al., 1989). However, the benzo-DPEP and benzo-etio porphyrins which were detected in the highest R_f fraction in pyrolysate 3 were not observed in the bitumen I because that R_f region was not investigated. This similarity in the porphyrin chromatographic patterns between the bitumen I and pyrolysate 3 is significant because it indicates that the VO(II) porphyrins generated from the kerogen closely resemble those of the solvent-extractable bitumen. The TLC fractions provide no evidence for the generation of substantial quantities of high carbon number VO(II) geoporphyrins or porphyrins of unusual skeletal types from the kerogen.

Comparison of the nickel and vanadyl porphyrin distributions

The distributions of the etio and DPEP porphyrins of the Ni(II) and VO(II) series in the New Albany bitumen I and kerogen pyrolysates are compared in

Fig. 6. The distributions of the two major porphyrin series (etio and DPEP) of the two metals are similar. The only major difference between the Ni(II) and VO(II) etio porphyrins is the displacement of the VO(II) etio distribution approximately one carbon number higher than the Ni(II) envelope in all samples studied, except for pyrolysate 5. Between 110 and 400°C, there is a shift in both distributions of approximately one carbon number to lower molecular weight. At 450°C, the shift to lower carbon numbers is more pronounced for both series and results from thermal dealkylation and/or selective thermal destruction of higher mass pseudo-homologs. Thus, the distributions are composed primarily of highly dealkylated species (C_{22}–C_{27} for Ni(II) and C_{23}–C_{28} for VO(II)). The only major difference between the two etio series is the broadened Ni(II) etio distribution (relative to the VO(II)) of pyrolysate 5 and the shoulder at C_{30}–C_{31}. Although this broadened distribution may be interpreted to result from conversion of Ni(II) DPEP to Ni(II) etio, there is no evidence for this conversion in the VO(II) porphyrin distributions. The carbon number ranges and C_{max} values of the Ni(II) and VO(II) DPEP distributions in the bitumen and in the pyrolysates are also similar.

Figure 7 compares the etio and DPEP distributions of the TLC fractions of pyrolysate 3. Although the solvent systems (and R_f ranges) used for the Ni(II) and VO(II) porphyrins were different, the distributions of both the etio and DPEP species of the metals are similar. In the case of the etio species, the VO(II) distributions are displaced to higher carbon numbers than the Ni(II) distributions in fractions A, B (one carbon) and E (two carbon numbers). For the DPEP series, the distributions have similar shapes and only in fraction E is the VO(II) distribution displaced to higher carbon number than the Ni(II) distribution.

Geochemical implications of porphyrin generation from kerogen during pyrolysis

The kerogen from the New Albany shale contains substantial concentrations of organically combined nickel and vanadium (36.3 and 13.7 μmol/g, respectively). Although the nature of all the nickel and vanadium species in the kerogen has not been determined, release of porphyrin complexes of both metals during pyrolysis of the kerogen between 110 and 450°C, in the presence of toluene, confirms that porphyrins are present in the kerogen. No non-porphyrin Ni(II) or VO(II) complexes identifiable by UV–visible spectrophotometry were observed. This observation substantiates previous geochemical studies that have inferred the generation of metalloporphyrins from kerogen during source-rock maturation (Mackenzie et al., 1980; Barwise and Roberts, 1984; Barwise, 1987; Baker and Louda, 1983, 1986a).

In this study, it has been shown that both the Ni(II) and VO(II) porphyrins generated from kerogens between 110 and 450°C are composed predominantly of etio and DPEP species with minor amounts of

THBD, BD, and BE species detected in the porphyrin concentrate of the 110°C pyrolysate only. That the Ni(II) and VO(II) porphyrins isolated from the bitumen I and the kerogen pyrolysates are very similar is evidenced by:

(i) The Ni(II) and VO(II) porphyrin concentrations in the pyrolysates show similar variations with pyrolysis temperature, with the maximum concentration for both species observed in pyrolysate 2 (210°C; Fig. 4). Also, the NiP/VOP ratio in the pyrolysates is essentially constant between 110 and 450°C and equal to the NiP/VOP ratios in the bitumen (Fig. 4a).

(ii) The variations in the rates of metalloporphyrin generation (μmol porphyrin/g kerogen TOC) with pyrolysis temperature show the same trends for both Ni(II) and VO(II), as shown in Fig. 5. The rate of generation increases from 110 to 400°C and peaks at 400°C beyond which severe thermal degradation of the porphyrins causes the net rate of generation to drop.

(iii) The carbon number distributions and C_{max} of the Ni(II) and VO(II) etio porphyrins in the pyrolysates are very similar except that the VO(II) etio distributions are displaced one carbon number higher. Similar distributions are observed from the New Albany bitumen I. The carbon number ranges and C_{max} of the Ni(II) and VO(II) DPEP porphyrins are similar in the bitumen and pyrolysates.

(iv) Alternate porphyrin series are observed in the porphyrin mixtures only in pyrolysate 1 [THBD for Ni(II); BD for VO(II)]. Minor amounts may be present in the other pyrolysates as was shown by TLC for pyrolysate 3.

(v) Fractionation of the Ni(II) and VO(II) porphyrins of pyrolysate 3 by TLC shows that both metalloporphyrin types have very similar R_f dependent distribution patterns and separate on the basis of carbon number, number of β-substituents, and skeletal type.

The similarity between the Ni(II) and VO(II) porphyrin distributions in the New Albany shale implies that metallation by both Ni^{2+} and VO^{2+} occurred with a common free-base porphyrin (or precursor) assemblage. Pyrolysis of New Albany shale kerogen has demonstrated that both metalloporphyrin types are associated with the kerogen and that simulated maturation releases larger amounts of Ni(II) porphyrin than VO(II) porphyrin at all pyrolysis temperatures. These conclusions are not consistent with the concept that the Ni(II) species form in a "free" or discrete state in the maturing sediment whereas the VO(II) species form in a kerogen associated state (Baker and Louda, 1983, 1986a). Additionally, in the case of the New Albany shale, there is no evidence that etio porphyrins are preferentially bound in the kerogen relative to the DPEP species. The DPEP/etio ratio of the VO(II) porphyrins is essentially constant between 110 and 400°C and decreases to zero at 450°C. At this temperature, decomposition of

the DPEP porphyrins and dealkylation of the etio porphyrins occurs. The DPEP/etio ratio of the Ni(II) species reaches a maximum value at 300°C and also decreased to zero at 450°C. These data demonstrate that DPEP porphyrins are associated with the kerogen. It is indeed not possible to determine whether either species is preferentially generated because the DPEP/etio ratios of the porphyrins in the kerogen cannot be determined. The decrease in the DPEP/etio ratio of the Ni(II) species above 300°C and of the VO(II) species above 400°C may be explained in at least three ways:

(i) DPEP porphyrins are converted thermally to etio species during pyrolysis (Corwin, 1960; Didyk et al., 1975), either in the kerogen itself or after release to the pyrolysate–solvent system.

(ii) DPEP porphyrins are preferentially degraded relative to etio (Barwise, 1987), either in the kerogen or the pyrolysate.

(iii) DPEP porphyrins are preferentially released relative to etio species at the lower temperature.

There is no evidence from the pyrolysis data that a DPEP to etio conversion occurs for the VO(II) porphyrins. For the VO(II) species, ring opening on the C_{28}–C_{33} DPEP porphyrins, which are the dominant DPEP species in the pyrolysates, should skew the etio distribution of the 450°C pyrolysate to carbon numbers higher than C_{26} (C_{max}), assuming that no carbons are lost in the conversion. There is no evidence that this is the case (Fig. 6). However, the broadening of the Ni(II) etio distribution and the shoulder at C_{30}–C_{31} in pyrolysate 5, concomitant with the sharp decrease in the DPEP/etio ratio from 300 to 400°C, implies a DPEP to etio conversion for the Ni(II) porphyrins. There is also no evidence of preferential release of DPEP relative to etio at lower temperatures. It is clear in the case of the VO(II) porphyrins that the DPEP/etio ratio remains essentially constant up to 400°C. The sharp decrease in the DPEP/etio ratio between 400 and 450°C appears to be the result of either the lower thermal stability of the DPEP species (i.e. thermal degradation) or preferential demetallation of DPEP by H_2S generated during the pyrolysis or a combination of these two effects.

Several studies have shown that biomarkers other than porphyrins are released during kerogen pyrolysis (Seifert, 1978; Burnham et al., 1982; Tissot, 1984; Lewan et al., 1979, 1986). The mechanisms of association of most biomarkers with the kerogen structure have not been determined, but bond rupture has been shown to play an important role in release from the kerogen matrix only at pyrolysis temperatures above 350°C (Seifert, 1978; Tissot, 1984) or at lower temperatures when catalytic mineral surfaces are present (Tannenbaum and Kaplan, 1985; Tannenbaum et al., 1986). Philp and Gilbert (1985) have concluded that some biomarkers (e.g. gammacerane) occur in kerogens by an association mechanism rather than by

direct chemical bonding. The association of the porphyrins with kerogens has been discussed by several authors (Mackenzie et al., 1980; Baker and Louda, 1983, 1986a; Barwise, 1987; Quirke et al., 1980; Filby and Van Berkel, 1987; Van Berkel and Filby, 1987). Baker and Louda (1983) proposed that the VO(II) porphyrins were combined in the kerogen by carbon–carbon linkages and that carbon–carbon bond rupture during catagenesis released porphyrins with a wide range of carbon numbers. Thus, kerogen association and release was proposed to account for porphyrin alkylation beyond that expected from chlorophyll precursors. Oehler et al. (1974) have shown that tetrapyrrole complexes can become grafted onto cellular macromolecules thus suggesting a mechanism for porphyrin precursors to become bonded to the kerogen structure. Quirke et al. (1980) suggested that porphyrin precursors could be incorporated into evolving kerogens in sediments by anti-Markovnikov addition to the vinyl group on the chlorophyll macrocycle. Other mechanisms proposed involve incorporation via ester linkages (Baker and Louda, 1986a). This study provides no experimental evidence that metalloporphyrins generated from the New Albany kerogen (and those in the bitumen) were chemically bonded to the kerogen. It should be stressed, however, that the nickel and vanadium species remaining in the kerogen after pyrolysis may be associated with the kerogen by a different mechanism from those porphyrins released during pyrolysis. Evidence from this study for a non-bonded association of the porphyrins with the kerogen includes the following:

(i) Over the pyrolysis temperature range 110–450°C, the highest concentrations of metalloporphyrins occur in the pyrolysate obtained at 210°C, a temperature at which carbon–carbon bond breaking is negligible (in the absence of mineral catalysts).

(ii) Ni(II) and VO(II) porphyrins are generated at an increasing rate (μmol/g kerogen TOC) with increasing temperature up to 400°C. Other than a shift of one carbon number in C_{max} of the etio species, there are virtually no differences in the etio metalloporphyrin distributions at these temperatures. If carbon–carbon bond breaking becomes an important mechanism of porphyrin generation at 400°C relative to other release mechanisms and is negligible at 110–210°C, there should be a qualitative change in the etio porphyrin distributions between 210 and 400°C. Similar conclusions may be reached for the Ni(II) and VO(II) DPEP porphyrins.

(iii) Except for the high carbon number VO(II) benzo DPEP porphyrins (C_{38}–C_{40}) present in the lowest temperature pyrolysate, there is no evidence for generation of high carbon number DPEP ($>C_{35}$) or etio ($>C_{33}$) porphyrins in significant amounts.

If the metalloporphyrins in the New Albany kerogen are not bonded to the kerogen via carbon–carbon bonds, other modes of association must be involved. These other modes of association might include:

(i) Physical trapping of metalloporphyrins in the kerogen structure. The porphyrins may be released when the kerogen matrix is dissolved by, or swells in, the solvent.

(ii) Chemisorption on the kerogen, either through π–π interactions of the porphyrin macrocycle with extended aromatic systems in the kerogen, or by bonding of specific heteroatom and other functional groups in the kerogen to the porphyrinic metal ion at the axial positions.

(iii) Concentration of the metalloporphyrins at the kerogen–mineral interface in the shales. On dissolution of the mineral matrix, the porphyrins may then associate with the kerogen by either process (i) or (ii).

Process (iii) may be an important one because of the known interfacial activities of metalloporphyrins (Moore and Dunning, 1955) and the importance of mineral surfaces in kerogen catagenesis.

Association of the metalloporphyrins with the New Albany kerogen may result from a combination of processes (i)–(iii). Generation of metalloporphyrins from kerogen at temperatures less than 300°C may result from increased solubility because of better solvent access within the kerogen structure (i.e. physical trapping) and a desorption of the porphyrins from kerogen surfaces into the solvent (toluene). There are no experimental data on the adsorption of metalloporphyrins on kerogens either from aqueous or from hydrocarbon solvents, but π–π interactions and axial ligand bonding (e.g. through N-donor groups) are likely modes of chemisorption. Possible evidence for a desorption mechanism is the displacement of the VO(II) etio distribution one carbon number higher than the corresponding Ni(II) etio distributions in both the bitumen and the pyrolysates (except possibly for pyrolysate 5). If the cyclic tetrapyrrolic precursors of the Ni(II) and VO(II) porphyrins are the same [as is indicated by the similarities in the Ni(II) and VO(II) distributions in the bitumen (Van Berkel et al., 1989) and pyrolysates], and if only a small proportion of the Ni(II) and VO(II) species are released from the kerogen during pyrolysis, porphyrin desorption at a given temperature should be determined by porphyrin polarity or affinity for the kerogen. Because the VO(II) etio porphyrins of a given carbon number are more polar than the corresponding Ni(II) species, desorption of similar polarity Ni(II) and VO(II) species at a given temperature would result in the observed displacement to higher carbon number of the VO(II) porphyrin distribution relative to the corresponding Ni(II) species.

Pyrolysate 1 (110°C) is probably composed primarily of residual bituminous material associated with the demineralized and solvent-extracted kerogen.
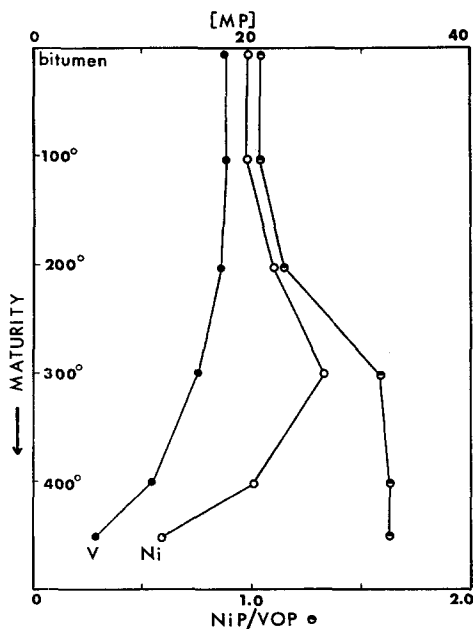
Fig. 8. Variation of Ni(II) (○) and VO(II) (●) porphyrin concentrations (MP in μmol/g) in bitumen of New Albany shale. Assumes original bitumen in rock and incremental addition at each pyrolysis temperature. Incremental pyrolysate and initial bitumen computed per gram TOC in shale.

Several workers have shown that the bitumen II in source rocks is different in composition and much more polar in nature than the bitumen I and is concentrated on mineral, primarily clay, surfaces (Spiro, 1984; Siskin et al., 1987). The polar nature of bitumen II is reflected in the lower NiP/VOP ratio relative to bitumen I or the pyrolysates (Table 2). Pyrolysate 1 has a lower NiP/VOP ratio than do the higher temperature pyrolysates or the original bitumens, implying that it is composed of bitumen II type material. Pyrolysate 1 is also unique among the pyrolysates in that it contains Ni(II) THBD and VO(II) BD porphyrins in sufficient amounts to be detected in the porphyrin concentrates. These alternate series porphyrins are present in much smaller concentrations in pyrolysate 3 and can be detected by EI-MS only after separation of the porphyrin mixtures into TLC fractions. The occurrence of the minor series in pyrolysate 1 implies that these species are probably concentrated in residual bitumen II and are desorbed, or released, from the kerogen at relatively low temperatures. This would imply that the alternate series may be associated primarily with the mineral matter in the New Albany shale, or occur at the kerogen–mineral interface, but are more tightly bound to the mineral matrix than are the DPEP and etio species.

Although it may be concluded that porphyrin generation from kerogen is primarily by desorption/ solubilization rather than carbon–carbon bond cleavage, thermal maturation of the porphyrins is likely to occur to a limited extent up to 400°C under the experimental conditions used. Above

400°C, thermolytic effects are of major importance. Thermal maturation of the metalloporphyrins can be recognized in:

(i) A decrease in the average mass, $\bar{M}$ (Table 3), of the etio porphyrin distributions from 110 to 450°C as a result of either dealkylation or preferential degradation of high carbon number etio species.

(ii) Degradation of the Ni(II) and VO(II) DPEP species at 450°C either by decomposition or demetallation.

If the pyrolysis sequence is considered as simulated geochemical maturation of the New Albany shale, then the variation in the Ni(II) and VO(II) porphyrin contents of an accumulating bitumen can be evaluated. Figure 8 shows the Ni(II) and VO(II) porphyrin contents and the NiP/VOP ratio of an accumulating bitumen, assuming an initial bitumen content of 6×10^{-2} g/g TOC for the New Albany shale and incremental addition of new bitumen at each pyrolysis stage calculated from the yields of the pyrolysates. The data show that the VO(II) porphyrin content decreases with increasing maturation while the Ni(II) porphyrin content reaches a maximum at a time–temperature region equivalent to 300°C pyrolysis temperature. The NiP/VOP ratio increases with maturation but beyond the maturation stage represented by 450°C (i.e. metagenesis) the ratio will decrease as shown by the trend in the NiP/VOP ratio with pyrolysis temperature (Fig. 4a).

CONCLUSIONS

Both Ni(II) and VO(II) porphyrins are associated with the kerogen of the New Albany shale. The Ni(II) and VO(II) porphyrin concentrations of the kerogen could not be determined, hence it is not certain whether one metal species is preferentially associated with the kerogen. Examination of the etio and DPEP porphyrin distributions of both Ni(II) and VO(II) allow the following conclusions to be reached:

(1) The porphyrins released during pyrolysis between 110 and 450°C appear to be desorbed or dissolved from the kerogen matrix rather than being released by carbon–carbon bond scission.

(2) The Ni(II) and VO(II) porphyrins released during pyrolysis have similar carbon number ranges and distribution patterns and thus appear to have been formed from common tetrapyrrole precursors. These precursors may have formed an association with the evolving kerogen prior to metallation. If this is the case, the metallation of the tetrapyrrole precursor may have occurred at the kerogen-mineral interface rather than in the solution state.

(3) After pyrolysis, the kerogens still contain significant amounts of organically combined nickel and vanadium. Whether these complexes are porphyrins which are not accessible to the solvent during

pyrolysis, or are bonded to the kerogen by carbon–carbon bonds, could not be determined. Non-porphyrin complexes which may be bonded to the kerogen or trapped in the kerogen structure may also be present.

(4) The kerogen appears to be the source of the Ni(II) and VO(II) porphyrins in the New Albany bitumen because the etio and DPEP distributions of the porphyrins in the bitumen are similar to those in the pyrolysates.

(5) The detection of Ni(II) THBD and VO(II) BD porphyrins in the porphyrin concentrate of only the 110°C pyrolysate indicates that the mineral matrix plays a role in their formation.

REFERENCES

Baker E. W. and Louda J. W. (1983) Thermal aspects in chlorophyll geochemistry. In *Advances in Organic Geochemistry 1981* (Edited by Bjorøy M. *et al.*), pp. 401–421. Wiley, Chichester.

Baker E. W. and Louda J. W. (1986a) Porphyrins in the geological record. In *Biological Markers in the Sedimentary Record* (Edited by Johns R. B.), pp. 125–225, Elsevier, Amsterdam.

Baker E. W. and Louda J. W. (1986b) Porphyrin geochemistry of Atlantic Jurassic–Cretaceous black shales. *Org. Geochem.* **10**, 905–914.

Baker E. W., Palmer S. E. and Huang W. Y. (1977) Intermediate and late diagenetic tetrapyrrole pigments, Leg 41: Cape Verde rise and basin. In *Initial Reports of the Deep Sea Drilling Project—XLI*, Vol. 41 (Edited by Lancelot Y., Siebold W. and the Shipboard Party), pp. 825–837. U.S. Government Printing Office, Washington D.C.

Baker E. W., Palmer S. E. and Huang W. Y. (1978) Chlorin and porphyrin geochemistry of DSDP Leg 40 sediments. In *Initial Reports of the Deep Sea Drilling Project—XL*, Vol, 40 (Edited by Bolli H. M., Ryan W. B. F. and the Shipboard Party), pp. 639–647. U.S. Government Printing Office, Washington, D.C.

Barwise A. J. G. (1987) Mechanisms involved in altering DPEP-etio porphyrin ratios in sediments and oils. In *Metal Complexes in Fossil Fuels* (Edited by Filby R. H. and Branthaver J. F.), pp. 100–109. American Chemical Society, Washington, D.C.

Barwise A. J. G., Evershed R. P., Wolff G. A., Eglinton G. and Maxwell J. R. (1986) High performance liquid chromatographic analysis of free-base porphyrins—I: An improved method. *J. Chromatogr.* **368**, 1–9.

Barwise A. J. G. and Roberts I. (1984) Diagenetic and catagenetic pathways for porphyrins in sediments. *Org. Geochem.* **6**, 167–176.

Burnham A. K., Clarkson J. E., Singleton M. F., Wong C. M. and Crawford R. W. (1982) Biological markers from Green River kerogen decomposition. *Geochim. Cosmochim. Acta* **46**, 1243–1251.

Chicarelli M. I., Kaur S. and Maxwell J. R. (1987) Sedimentary porphyrins: unexpected structures, occurrence and

possible origins. In *Metal Complexes in Fossil Fuels* (Edited by Filby R. H. and Branthaver J. R.), pp. 40–67. American Chemical Society, Washington, D.C.

Corwin A. H. (1960) Petroporphyrins. Paper V-10, *5th World Petroleum Congr.*, New York, pp. 119–129.

Didyk B. M., Alturki Y. I. A., Pillinger C. T. and Eglinton G. (1975) Petroporphyrins as indicators of geothermal maturation. *Nature* **256**, 563–565.

Filby R. H. and Van Berkel G. J. (1987) Geochemistry of metal complexes in petroleum, source rocks, and coals: an overview. In *Metal Complexes in Fossil Fuels* (Edited by Filby R. H. and Branthaver J. F.), pp. 2–38. American Chemical Society, Washington, D.C.

Lewan M. D., Bjorøy M. and Dolcater D. L. (1986) Effects of thermal maturation of steroid hydrocarbons as determined by hydrous pyrolysis of Phosphoria Retort shale. *Geochim. Cosmochim. Acta* **50**, 1977–1988.

Lewan M. D., Winters J. C. and McDonald J. H. (1979) Generation of oil-like pyrolysates from organic-rich shales. *Science* **203**, 847–849.

Mackenzie A. S., Quirke J. M. E. and Maxwell J. R. (1980) Molecular parameters of maturation in the Toarcian shales, Paris Basin, France—II. Evolution of metalloporphyrins. In *Advances in Organic Geochemistry 1979* (Edited by Douglas A. G. and Maxwell J. R.), pp. 239–248. Pergamon Press, Oxford.

McKay J. R. (1984) A discussion of the chemical structure of the organic matter in Green River oil shale. *Energy Sources* **7**, 257–270.

Moore J. W. and Dunning H. N. (1955) Interfacial activities and porphyrin oil shale extracts. *Ind. Engng Chem.* **47**, 1440–1444.

Ocampo R., Callot H. J. and Albrecht P. (1987) Evidence for porphyrins of bacterial and algal origin in oil shale. In *Metal Complexes in Fossil Fuels* (Edited by Filby R. H. and Branthaver J. R.), pp. 68–73. American Chemical Society, Washington, D.C.

Oehler J. H., Aizenshtat Z. and Schopp W. J. (1974) Thermal alteration of blue-green algae and blue-green algal chlorophyll. *Am. Assoc. Pet. Geol. Bull.* **58**, 124–132.

Palmer S. E. and Baker E. W. (1978) Copper porphyrins in deep-sea sediments: a possible indicator of oxidized terrestrial organic matter. *Science* **201**, 49–51.

Philp R. P. and Gilbert T. D. (1985) Source rock and asphaltene biomarker characterization by pyrolysis–gas chromatography–mass spectrometry–multiple ion detection. *Geochim. Cosmochim. Acta* **49**, 1421–1432.

Quirke J. M. E. (1987) Techniques for isolation and characterization of the geoporphyrins and chlorins. In *Metal Complexes in Fossil Fuels* (Edited by Filby R. H. and Branthaver J. R.), pp. 308–331. American Chemical Society, Washington, D.C.

Quirke J. M. E., Cuesta L. L., Yost R. A., Johnson J. V. and Britton E. D. (1989) Studies on high carbon number geoporphyrins by tandem mass spectrometry. *Org. Geochem.* **14**, 43–50.

Quirke J. M. E., Eglinton G. and Maxwell J. R. (1979) Petroporphyrins—I: a preliminary characterization of the porphyrins of gilsonite. *J. Am. Chem. Soc.* **101**, 7693–7697.

Quirke J. M. E., Eglinton G., Palmer S. E. and Baker E. W. (1982) High performance liquid chromatography and mass spectrometric analysis of porphyrins from deep-sea sediments. *Chem. Geol.* **35**, 69–85.

Quirke J. M. E., Shaw G. J., Soper P. D. and Maxwell J. R. (1980) Petroporphyrins—II: the presence of porphyrins with extended alkyl substituents. *Tetrahedron* **35**, 3261–3267.

Rankel L. A. (1987) Degradation of metalloporphyrins in heavy oils before and during processing: effects of heat, air, hydrogen, and hydrogen sulfide on petroporphyrin species. In *Metal Complexes in Fossil Fuels* (Edited by

Filby R. H. and Branthaver J. R.), pp. 257–264. American Chemical Society, Washington, D.C.

Riley K. W. and Saxby J. D. (1982) Association of organic matter and vanadium in oil shale from the Toolebuc Formation of the Eromanga Basin of Australia. *Chem. Geol.* **37**, 265–275.

Seifert W. K. (1978) Steranes and terpanes in kerogen pyrolysis for correlation of oil and source rocks. *Geochim. Cosmochim. Acta* **42**, 473–484.

Siskin M., Brons G. and Payack J. F. (1986) Disruption of kerogen-mineral interactions in oil shales. *Am. Chem. Soc. Div. Pet. Chem. Preprints* **32**, 75–79.

Smith K. M. (1975) *Porphyrins and Metalloporphyrins*, p. 884. Elsevier, Amsterdam.

Spiro B. (1984) Effects of the mineral matrix on the distribution of geochemical markers in thermally affected sedimentary sequences. *Org. Geochem.* **6**, 543–560.

Spiro B., Dinur D. and Aizenshtat Z. (1983) Evaluation of source, environment of deposition, and diagenesis of some Israeli oil shales, n-alkanes, fatty acids, tetrapyrroles and kerogen. *Chem. Geol.* **39**, 189–214.

Sundararaman P. (1985) High performance liquid chromatography of vanadyl porphyrins. *Anal. Chem.* **57**, 2204–2206.

Tannenbaum E., Huizinga B. J. and Kaplan I. R. (1986) Role of minerals in thermal alteration of organic matter—II: a material balance. *Bull. Am. Assoc. Pet. Geol.* **70**, 1156–1165.

Tannenbaum E. and Kaplan I. R. (1985) Role of minerals in the thermal alteration of organic matter—I: generation of gases and condensates under dry conditions. *Geochim. Cosmochim. Acta* **49**, 2589–2604.

Tissot B. P. (1984) Recent advances in petroleum geochemistry applied to hydrocarbon exploration. *Bull. Am. Assoc. Pet. Geol.* **68**, 545–563.

Tissot B. P. and Welte D. H. (1984) *Petroleum Formation and Occurrence*, 2nd edn, p. 699. Springer, Berlin.

Treibs A. (1936) Chlorophyll and hemin derivatives in organic mineral substances. *Angew. Chem.* **49**, 682–686.

Van Berkel G. J. (1987) The role of kerogen in the origin and evolution of nickel and vanadyl geoporphyrins. Ph.D. Dissertation, Washington State University, Pullman, Wash.

Van Berkel G. J. and Filby R. H. (1987) Generation of nickel and vanadyl porphyrins from kerogen during simulated catagenesis. In *Metal Complexes in Fossil Fuels* (Edited by Filby R. H. and Branthaver J. F.), pp. 110–134. American Chemical Society, Washington, D.C.

Van Berkel G. J. and Filby R. H. (1988) Determination of the mineral-free nickel and vanadium contents of Green River oil-shale kerogen. In *Geochemical Biomarkers* (Edited by Yen T. F. and Moldowan J. M.), pp. 89–114. Harwood, Chur, Switzerland.

Van Berkel G. J., Quirke J. M. E. and Filby R. H. (1989) The Henryville Bed of the New Albany shale—I. Preliminary characterization of the nickel and vanadyl porphyrins in the bitumen. *Org. Geochem.* **14**, 119–128.